Available online at www.sciencedirect.com
ScienceDirect
Earth and Planetary Science Letters 251 (2006) 18–32
EPSL
www.elsevier.com/locate/epsl

High-resolution data of the Iceland Basin geomagnetic excursion from ODP sites 1063 and 983: Existence of intense flux patches during the excursion?

Mads Faurschou Knudsen *, Conall Mac Niocaill, Gideon M. Henderson

Department of Earth Sciences, University of Oxford, Parks Road, Oxford, OX1 3PR, United Kingdom

Received 7 April 2006; received in revised form 11 August 2006; accepted 17 August 2006
Available online 2 October 2006
Editor: H. Elderfield

Abstract

Based on discrete samples, we report new high-resolution records of the ~ 185 kyr Iceland Basin (IB) geomagnetic excursion from Ocean Drilling Project (ODP) Site 1063 on the Bermuda Rise (sedimentation rate 32 cm kyr^{-1}) and from ODP Site 983 in the far North Atlantic (sedimentation rate 18 cm kyr^{-1}). Two records from Holes 1063A and 1063B are very consistent, and provide the highest resolution of the detailed field behaviour during the IB excursion obtained so far. Inclination records from Holes 983B and 983C in the far North Atlantic are also very consistent, whereas declination anomalies deviate more notably. The pseudo-Thellier (PT) technique was applied along with more conventional palaeointensity proxies (NRM/ARM and NRM/κ) to recover relative palaeointensity (RPI) estimates from Hole 1063A and Hole 983B. As expected, these proxies indicate that the field intensity generally dropped at both sites during the IB excursion, but also that the history of RPI from the two sites is different.

VGPs from Site 1063 indicate that the field at this location experienced some stop-and-go behaviour between patches of intense vertical flux over North America and the tip of South America, areas which coincide fairly well with patches of preferred transitional VGP clustering from reversals and zones of high seismic velocity in the lower mantle. Changes in RPI at this location were generally gradual, possibly due to the proximity of these flux patches, and the first period of VGP-clustering over North America was accompanied by a conspicuous increase in RPI. VGPs from Site 983 track along a different path, and the associated RPI changes are very abrupt and completely synchronous with the onset and termination of the excursion. The differing VGP paths from Sites 1063 and 983 indicate that the global field structure during the IB excursion was not dominated by a single dipole.

Keywords: Geomagnetic excursions; Iceland Basin excursion; Preferred VGP longitudes; Patches of vertical flux; Geomagnetic field structure

1. Introduction

Compilations of palaeomagnetic records have established that geomagnetic excursions (defined as periods when the virtual geomagnetic poles (VGPs) deviate more than 45° from the geographic poles) are an intrinsic part of Earth's magnetic field behaviour. Up to 12 such excursions have been proposed for the interval since the last full geomagnetic reversal 780,000 yrs ago [1]. The duration of such geomagnetic excursions is not well-defined, but estimates of Brunhes-aged excursions range from 1000 to 3000 yrs [2,3] to as long as

* Corresponding author. Tel.: +44 0 1865 282 117; fax: +44 0 1865 272 072.
E-mail address: madsk@earth.ox.ac.uk (M.F. Knudsen).

0012-821X/$ - see front matter © 2006 Elsevier B.V. All rights reserved.
doi:10.1016/j.epsl.2006.08.016

10,000 yrs [4]. Constraining the duration of these events is important because it has been suggested that excursions arise when the field reverses polarity in the liquid outer core, and subsequently returns to the original polarity state before the field reversal propagates to the solid inner core [5]. Field changes in the outer core are dominated by convection with timescales of ~ 500 yrs, whereas field changes in the inner core are dictated by diffusion with a timescale of ~ 3000 yrs [6].

Geomagnetic excursions and full polarity reversals have recently been the focus of increasing attention, since they play a key role in the study of the fundamental processes controlling field generation in Earth's interior (e.g. [5,7–10]). Despite increasing efforts, which include integration of palaeomagnetic observations and numerical simulations (e.g. [11,12]), questions regarding the fundamental character of geomagnetic excursions still remain unanswered. For example, it is still unknown whether the field structure during excursions is predominantly dipolar or non-dipolar. One hindrance in this pursuit is the scarcity of reliable, high-resolution records of geomagnetic excursions. The resolution and fidelity of the records are often insufficient to resolve the detailed field behaviour during the excursions. Other problems relate to difficulties in correlating records from different regions, not to mention records from the same area, and to the fact that many excursions are missing in most sediment records. Generally, a relatively high sedimentation rate (preferably above 10 cm kyr^{-1}) is required to faithfully capture the rapidly changing field during an excursion [13], and sedimentary environments often fail to document excursions due to smoothing of the magnetic signal. Lavas provide a more reliable record of the

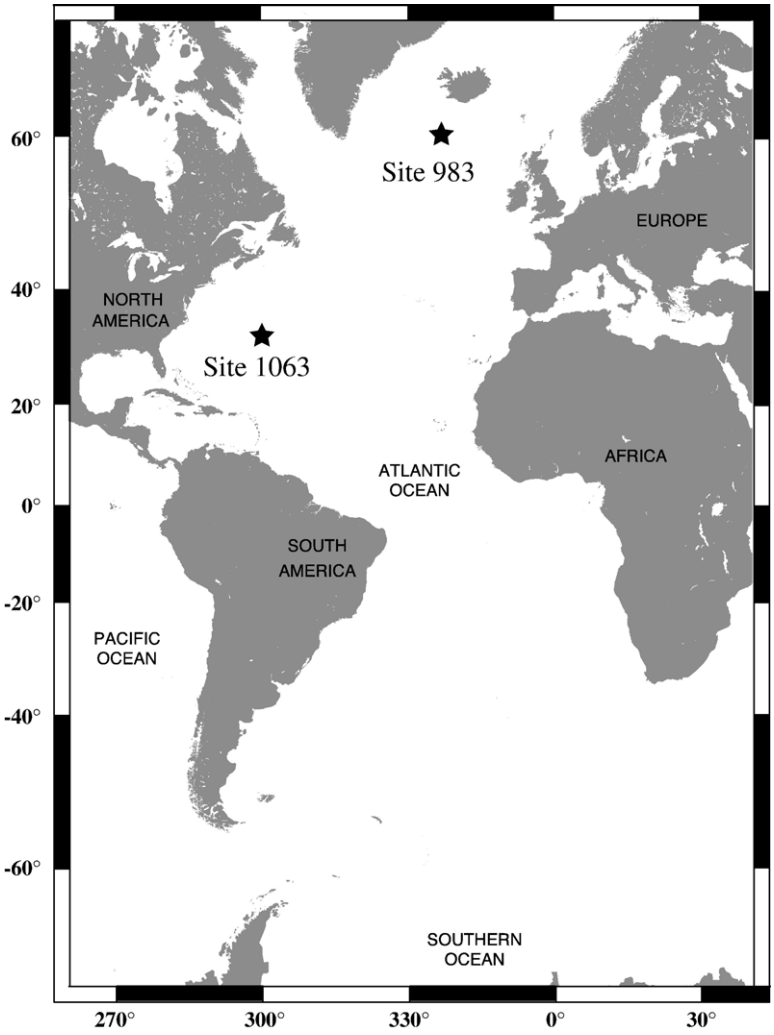

Fig. 1. Location of ODP Site 1063 (33.7°N, 57.6°W) and ODP Site 983 (60.4°N, 23.6°W).

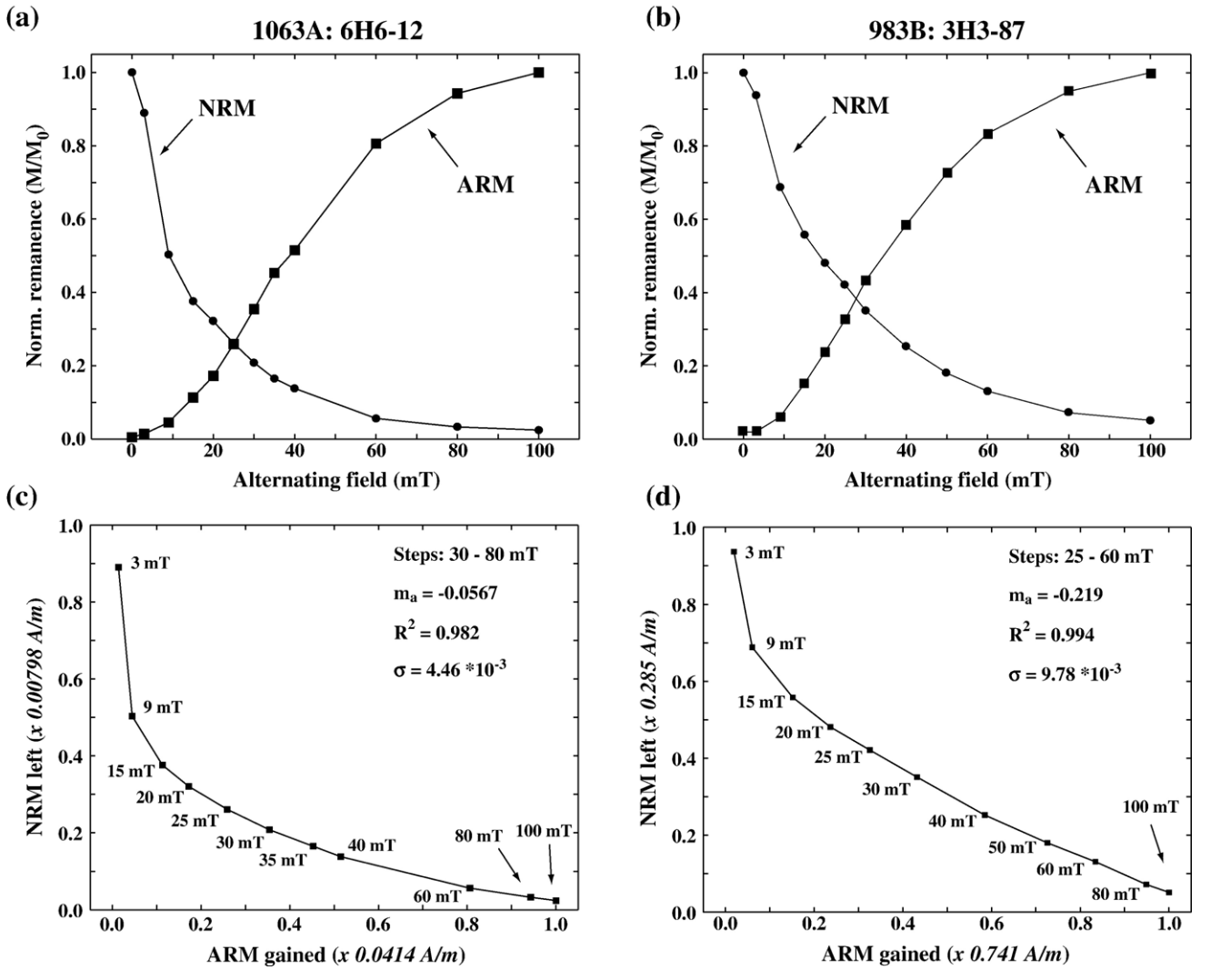

Fig. 2. Examples of the pseudo-Thellier technique applied to samples 6H6-12 from 1063A (a and c) and 3H3-87 from 983B (b and d). (a) and (b) show the normalised NRM demagnetisation and ARM acquisition versus field steps used for the pseudo-Thellier analysis. Note that the ARM was acquired using 12 of the 17 steps that were applied in the AF demagnetisation of the NRM (1063A: 0, 3, 9, 15, 20, 25, 30, 35, 40, 60, 80, 100 mT and 983B: 0, 3, 9, 15, 20, 25, 30, 40, 50, 60, 80, 100 mT). (c) and (d) show the NRM intensity left versus the acquired ARM intensity after each field step. m_a is the best-fit slope, and hence the PT-RPI estimate, σ the standard error of the slope used to calculate the uncertainty ($\pm 2\sigma$). The standard errors of the slopes were generally small compared to the resultant PT-RPI estimates.

magnetic field than sediments, but the temporal resolution is discontinuous and often very sparse.

The Iceland Basin (IB) excursion was named after a geomagnetic excursion observed in U-channel data from ODP Site 983 in the North Atlantic, and it was constrained to the interval 186–189 kyr by $\delta^{18}O$ tuning [14,15]. Despite being one of the best documented excursions in the literature (e.g. [16–20,4,21]), very few high-resolution records of the IB excursion exist. In this study we present new high-resolution records of the rapidly changing field

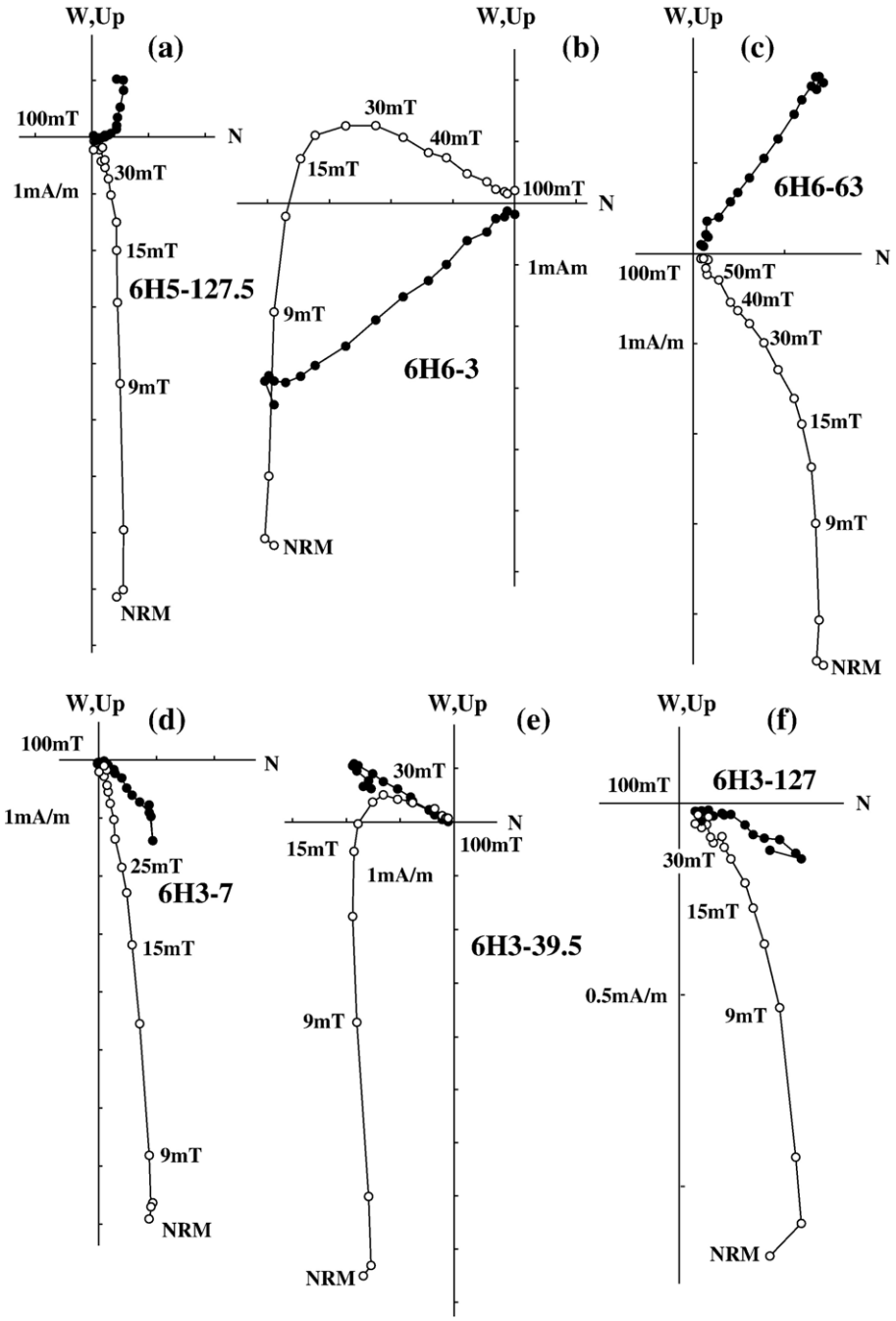

Fig. 3. Typical examples of vector endpoint diagrams. Solid (open) symbols represent projection of the vector onto a horizontal (vertical) plane. (a–c) Diagrams from Hole 1063A, (d–f) from Hole 1063B, (g–j) from Hole 983B, and (k–l) from Hole 983C. Diagrams b, e, h, and l are from samples within the excursion intervals.

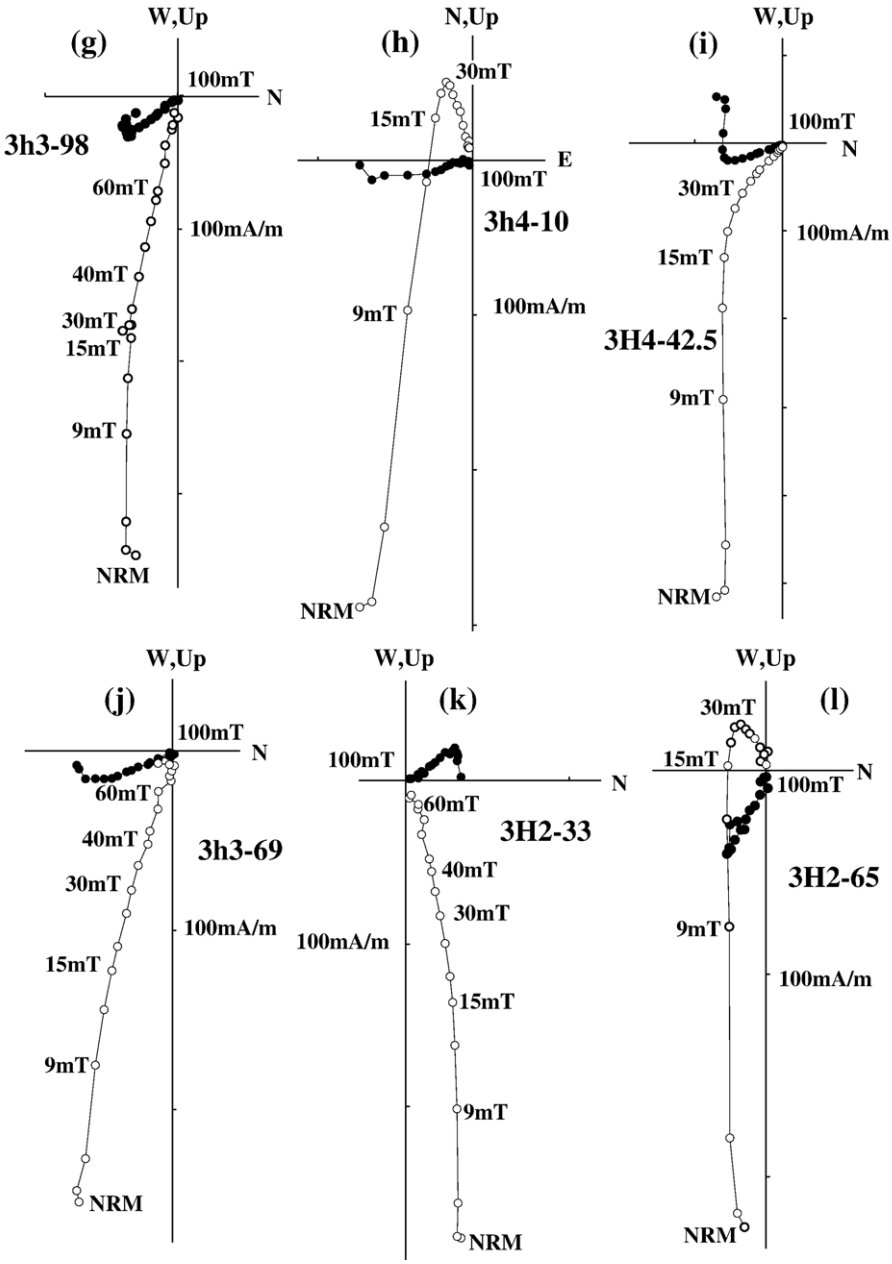

Fig. 3 (*continued*).

and relative palaeointensity during the Iceland Basin (IB) excursion from Ocean Drilling Program (ODP) Site 1063 on the Bermuda Rise. These records, based on discrete samples from sediments with an average sedimentation rate of 32 cm kyr^{-1}, provide the highest resolution of the IB excursion obtained so far. We furthermore present discrete-sample records of the IB excursion from two holes cored at Site 983 (average sedimentation rate 18 cm kyr^{-1}).

2. Sedimentology and stratigraphy

Site 1063 was cored during ODP Leg 172 in drift deposits from the northeast Bermuda Rise (Fig. 1). Holes 1063A and 1063B, cored at water depths of ~ 4584 m, have similar lithologies and meet the requirements for high-resolution palaeoceanographic and palaeomagnetic studies [1]. The dominant lithology of the subunit studied here is light grey to greenish grey

clay with varying proportions of silt and carbonate- and siliceous-bearing nannofossils. The predominance of clay at Site 1063 is in accordance with the Bermuda Rise being shaped by advection of fine-grained, abyssal sediments onto the plateau by deep bottom currents [22]. Shipboard long-core and U-channel palaeomagnetic data suggest that up to 11 Brunhes-aged excursions were recorded at Site 1063, indicating that these sediments are reliable recorders of the palaeomagnetic field [1].

Site 983, ODP Leg 162, was located on the Gardar Drift south of Iceland (Fig. 1). Holes 983B and 983C were cored at water depths of ~ 1985 m on the eastern flank of the Reykjanes Ridge. The sediments at Site 983 are predominantly composed of rapidly accumulated, fine-grained terrigenous particles with minor amounts of carbonate and biosilica. The high content of volcanic, terrigenous material from Iceland makes these sediments very suitable for palaeomagnetic studies, as documented in several earlier publications [14,15,23].

2.1. Chronologies and sedimentation rates

The IB excursion is quite easily correlated among records from different sites, because it is coeval with an abrupt change in climate and so can be unequivocally identified. Observed geomagnetic excursions can be correlated by comparison with the global δ^{18}O-curve (e.g. SPECMAP [24,25]), relying on the fact that the IB excursion is synchronous with the transition between marine oxygen isotope stages (MIS) 7 and 6 [15]. The δ^{18}O-record for Site 1063 contains many gaps, but the existing records of magnetic susceptibility [26] display a pattern very similar to δ^{18}O-variations in the SPECMAP-curve, and the IB excursion coincides with the transition between MIS 7 and 6 at 188 kyr. The mean sedimentation rate in the interval that recorded the IB excursion at Site 1063 is ~ 32 cm kyr^{-1}, the highest sedimentation rate reported for any record of this excursion.

At Site 983, detailed correlation between the existing δ^{18}O-stratigraphy [27] and the SPECMAP curve provides a reliable age model for this site. As for Site 1063, the IB excursion recorded at Site 983 coincides with the transition between MIS 7 and 6. The mean sedimentation rate in the interval encompassing the IB excursion is also high (~ 18 cm kyr^{-1}).

3. Methods

Based on published long-core and U-channel data we selected sediment cores from the Bermuda Rise (Site 1063, ODP Leg 172) and far North Atlantic (Site 983, ODP Leg 162) to make a comparative, high-resolution study of the geomagnetic-field behaviour during the IB excursion. At the ODP core repository in Bremen, we collected 41 discrete samples (7 cm^3) from the interval 53.48–55.43 mcd (meters composite depth) in core 1063A and 34 from 1063B (53.56–55.32 mcd). From the Gardar Drift in the North Atlantic, we collected 80 discrete samples from the interval 19.22–22.04 mcd in core 983B and 22 from core 983C (20.18–21.42 mcd).

Measurements of anisotropy of magnetic susceptibility (AMS) were performed on all discrete samples, using the KLY2 Kappabridge in the Palaeomagnetic Laboratory, Oxford University, in order to be able to rule

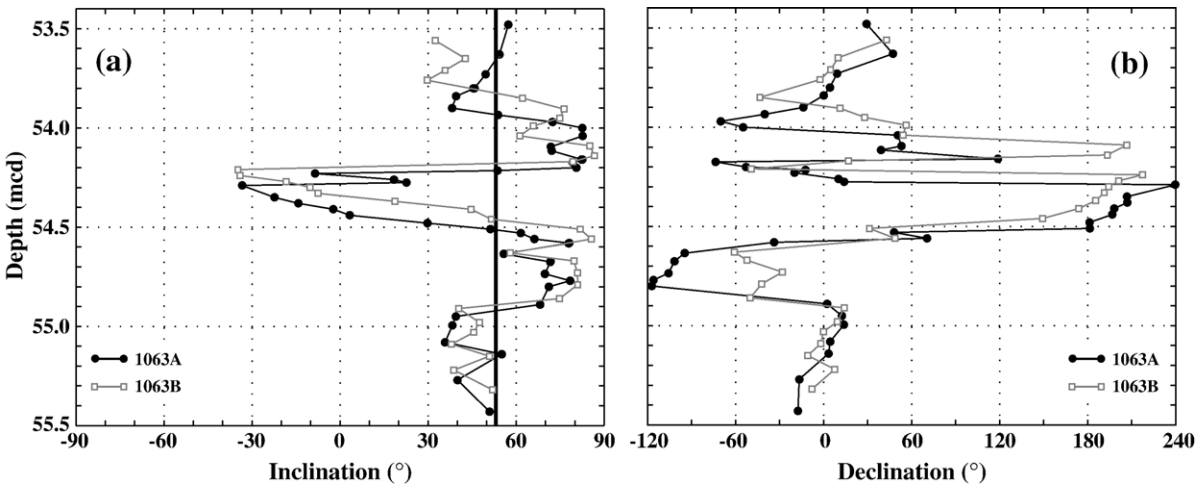

Fig. 4. New high-resolution records of the Iceland Basin excursion from the Central Atlantic. (a) Component inclinations and (b) declinations after AF demagnetisation and PCA of discrete samples from Holes 1063A (circles) and 1063B (squares), plotted on the composite depth scale for Site 1063 (33.7°N, 57.6°W) on the Bermuda Rise (ODP Leg 172).

out strong influence from variations in magnetic fabric on the observed directions. Subsequently, all samples were subjected to stepwise alternating-field (AF) demagnetisation of the natural remanent magnetisation (NRM) at applied fields of 0, 3, 6, 9, 12, 15, 20, 25, 30, 35, 40, 50, 60, 70, 80, 90, and 100 mT. Measurements and demagnetisation of the NRM were performed with a fully automated 2G Enterprises DC-SQUID Cryogenic Magnetometer with an in-line, triaxial alternating field (AF) demagnetiser. Principal component analysis (PCA) was used to determine the characteristic remanent magnetisation (ChRM).

3.1. Relative palaeointensity and the pseudo-Thellier technique

The conventional method for extracting information about variations in palaeointensity in sediments relies on normalization of NRM intensities by a parameter that compensates for changes in magnetic grain size and concentration. The most commonly used normalisers are the anhysteretic remanent magnetisation (ARM), isothermal remanent magnetisation (IRM), and the magnetic susceptibility (κ). Susceptibility is usually not the preferred normaliser, since some magnetic grains, such as large multi-domain magnetite grains or paramagnetic and superparamagnetic grains, may contribute to the susceptibility but not the remanence. Apart from using the conventional "brute force" methods, NRM/ARM and NRM/κ, as palaeointensity proxies, we additionally used the more reliable pseudo-Thellier (PT) method in order to minimize possible contributions of viscous remanent magnetisation (VRM) to the NRM. Another advantage of the PT technique is that it provides an estimate of the uncertainty associated with each individual relative palaeointensity (RPI) determination [28]. Samples from Hole 1063A (41 samples) and Hole 983B (80 samples) were used to determine RPI variations during the IB excursion. ARM acquisitions and subsequent demagnetisations were undertaken in the Palaeomagnetic and Mineral Magnetic Laboratory at the GeoBiosphere Science Centre, University of Lund, Sweden, using a 2G Enterprises model 755-R SQUID magnetometer, equipped with automated AF coils and a DC bias coil.

We followed the method proposed by Tauxe et al. [28] for application of the PT technique, a method also used in other detailed RPI studies (e.g. [29,30]). Subsequent to AF demagnetisation of the NRM, each specimen from 1063A and 983B was subjected to acquisition of ARM in stepwise increasing AF fields with a 0.05 mT direct-current bias field. The demagnetisation of the NRM and subsequent ARM acquisition are illustrated in Fig. 2a and b for two samples from 1063A and 983B, respectively. A large fraction of the NRM intensity is lost after demagnetisation at low fields, indicating that low-coercivity magnetic grains contribute significantly to the NRM intensity. Using the PT technique, an estimate of the relative palaeointensity (PT-RPI) is obtained by plotting the NRM intensity left after demagnetisation versus the acquired ARM intensity (Fig. 2c and d) and by linear regression determine the best-fit slope, m_a, relating the NRM and ARM between two field steps. Data that lie along a curve were avoided in the regression analyses, as these have been taken to represent removal of VRM [28]. Data used to determine the best-fit slope, and hence the PT-RPI, was selected through a combination of statistical analysis, optimizing the goodness-of-fit of the line to the data, m_a/σ, where σ is the standard error of the slope

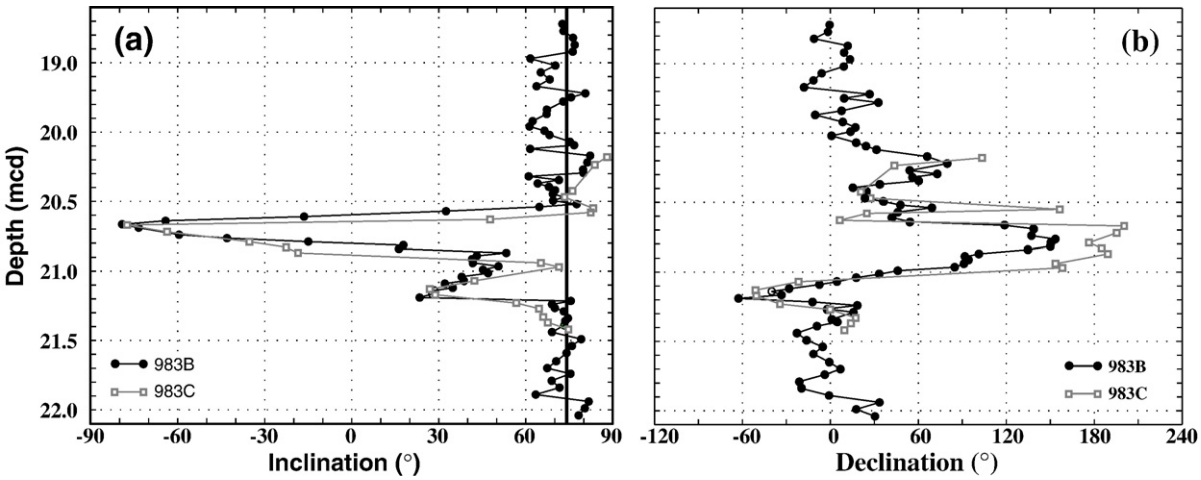

Fig. 5. High-resolution records of the Iceland Basin excursion from the North Atlantic. (a) Component inclinations and (b) declinations for Holes 983B (circles) and 983C (squares), plotted on the composite depth scale for Site 983 (60.4°N, 23.6°W), ODP Leg 162.

[28,31], and an attempt to use as large a portion of the NRM as possible without including contributions from VRM. Based on maximizing m_a/σ and including a minimum of 4 data points, data from intervals 30–80 mT and 25–60 mT were found to give the optimal fitting regression line for samples from 1063A and 983B, respectively. The uncertainty associated with each individual PT-RPI estimate is given by $\pm 2\sigma$ [28].

The ARM acquired at 100 mT AF was demagnetised in order to compute the conventional NRM/ARM palaeointensity proxy. For samples from 1063A (983B), values of NRM/ARM were computed after demagnetisation at 25 and 30 mT (25 and 40 mT), since this proved sufficient to eliminate the steep secondary overprint associated with the drilling process (Fig. 3). Finally, the values of $NRM_{25\ mT}/\kappa$ were computed for all samples from 1063A and 983B.

4. Results

The AMS measurements reveal that anisotropy of the magnetic fabric is negligible throughout the cores. Orthogonal projections of progressive AF demagnetisation data indicate the presence of a steep secondary overprint, probably a coring-induced overprint, in the majority of samples (Fig. 3). Typical vector-endpoint diagrams reveal that the stable, primary magnetisation components generally were easily isolated after removal of this overprint by AF demagnetisation at peak fields above 12–25 mT (Fig. 3). For all samples, the ChRM component was computed by principal component analysis (PCA). Maximum angular deviation (MAD) values for the remanence components from Site 983 are generally below 5°, whereas the MAD-values for Site 1063 are slightly higher with ~ 50% of the ChRM components having MADs below 5°. The small difference in the level of MAD-values between Site 1063 and Site 983 may be related to the fact that the NRMs are higher in samples from Site 983 than in samples from Site 1063.

4.1. Directional results

The ODP drill cores are not oriented and absolute declination values are thus impossible to derive from measurements alone. We use the standard approach to

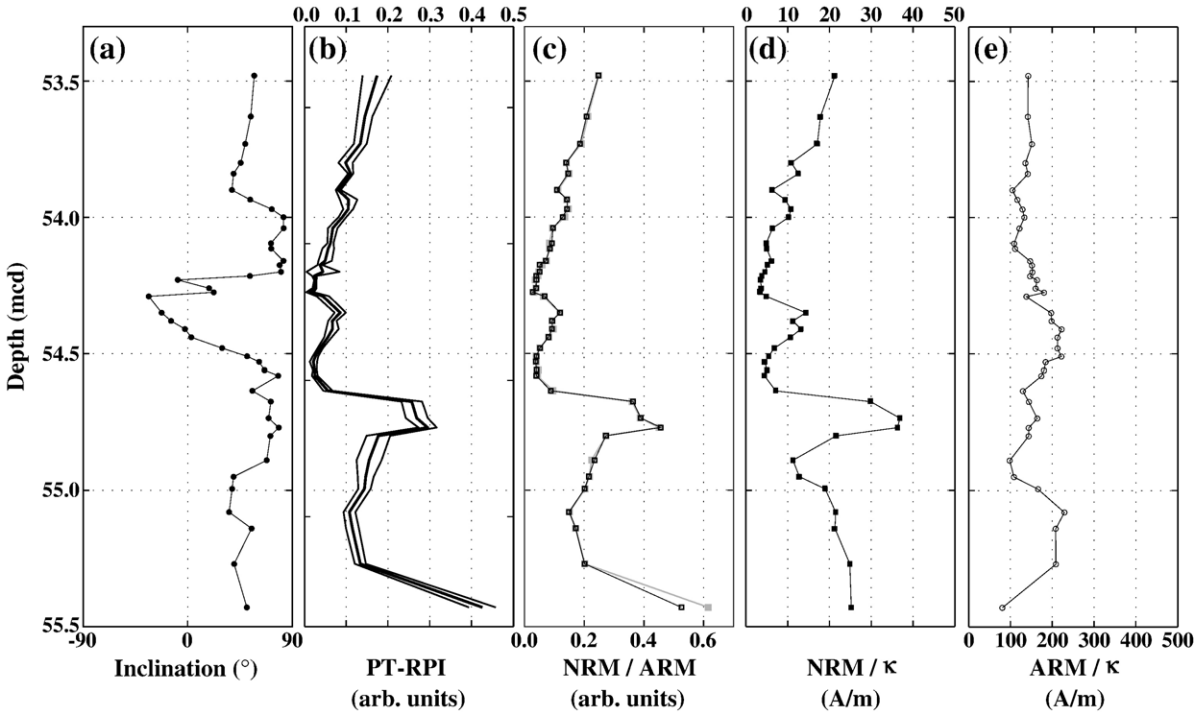

Fig. 6. Estimates of the relative palaeointensity during the IB excursion from 1063A along with (a) component inclinations for comparison. (b) PT-RPI (bold line) and the associated uncertainties $\pm 2\sigma$ (thin lines). PT-RPI values obtained from the regression analyses are multiplied by −1. Also shown are RPI estimates obtained by the conventional methods (c) $NRM_{25\ mT}/ARM_{25\ mT}$ (grey) and $NRM_{30\ mT}/ARM_{30\ mT}$ (black) along with (d) $NRM_{25\ mT}/\kappa$. (e) The magnetic grain-size proxy $ARM_{100\ mT}/\kappa$. Note that (d) and (e) are plotted on equivalent scales to make comparisons between relative changes in $NRM_{25\ mT}/\kappa$ and $ARM_{100\ mT}/\kappa$ more straightforward.

overcome this by reorienting core-segments until declinations from samples not included in the excursion interval average to a declination of 0°.

The inclinations (Fig. 4a) and declinations (Fig. 4b) from Holes 1063A and 1063B on the Bermuda Rise are plotted on the composite depth scale for Site 1063 (see Supplementary data). The slight misalignment of the curves from 1063A and 1063B probably arises from subtle differences in the depth models for the two holes. Alternatively, but less likely, this misalignment could arise from local differences in palaeomagnetic lock-in depth, as observed in sediment cores from Salerno Gulf, Italy [32]. While the two inclination curves are very similar (Fig. 4a), declinations differ more notably (Fig. 4b). The disagreement between the two declination records is most pronounced during the high-inclination intervals, especially the lower of the two (54.5–55.0 mcd) where misalignment cannot account for the differences observed, when declination is expected to become less reliably determined. Both inclination curves from Site 1063 show that the inclination increases to ~ 80° before it rapidly drops to negative values around −30°. After this negative trough, the inclination rapidly swings back to very high inclinations around 80–85° before it finally returns to the expected value for this location. The two inclination "shoulders" on either side of the excursion peak, where the field is very steep, are very conspicuous in both records from Site 1063. The initial increase to high inclinations is associated with a simultaneous change in declination values. During the excursion peak, characterised by negative inclinations, declination values swing to ~ 180° before they again become more scattered during the second high-inclination period following the excursion peak.

Inclinations (Fig. 5a) and declinations (Fig. 5b) from Holes 983B and 983C are plotted on the composite depth scale for Site 983 (see Supplementary data). As for Site 1063, any misalignment of the curves from 983B and 983C most likely arise from differences in the depth models for the two holes. The two inclination curves from 983B and 983C are in excellent agreement, showing that a small anomaly, with inclinations dropping to ~ 30°, preceded a large negative peak with inclinations reaching −80°. The declination curves from 983B and 983C differ somewhat throughout the excursion, but nevertheless seem to agree on the overall

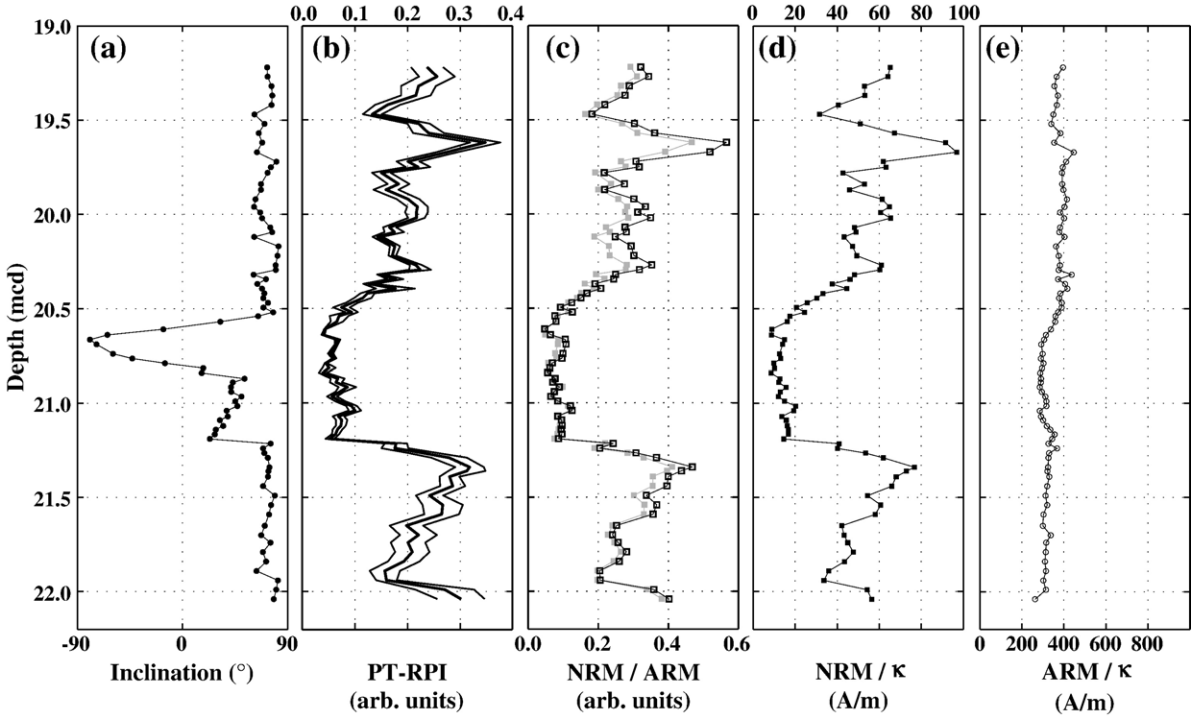

Fig. 7. Estimates of the relative palaeointensity during the IB excursion from 983B along with (a) component inclinations for comparison. (b) PT-RPI (bold line) and the associated uncertainties ±2σ (thin lines). PT-RPI values obtained from the regression analyses are multiplied by −1. Also shown are RPI estimates obtained by the conventional methods (c) $NRM_{25\ mT}/ARM_{25\ mT}$ (grey) and $NRM_{40\ mT}/ARM_{40\ mT}$ (black) along with (d) $NRM_{25\ mT}/\kappa$. (e) The magnetic grain-size proxy $ARM_{100\ mT}/\kappa$. Note that (d) and (e) are plotted on equivalent scales to make comparisons between relative changes in $NRM_{25\ mT}/\kappa$ and $ARM_{100\ mT}/\kappa$ more straightforward.

trends during the excursion. Directions obtained from discrete samples in this study agree very well with directions derived from earlier U-channel measurements from the same holes [15].

Based on correlation between existing age models and the intervals encompassing the directional anomalies, the estimated age of the IB excursion is 185–188 kyr at Site 1063 and 186–189 kyr at Site 983. When the inclination shoulders from Site 1063 are included in the interval encompassing the excursion (which is correct as the VGP latitudes generally are below 45°) the estimated duration of IB excursion is ~ 3 kyr, which is very similar to the duration estimated from Site 983.

4.2. Relative palaeointensity estimates

PT-RPI estimates from 1063A are shown in Fig. 6b along with the associated uncertainty ($\pm 2\sigma$), whereas the conventional palaeointensity proxies, NRM/ARM ($NRM_{25\ mT}/ARM_{25\ mT}$ and $NRM_{30\ mT}/ARM_{30\ mT}$) and $NRM_{25\ mT}/\kappa$, are shown in Fig. 6c and d. It is reassuring that the three different palaeointensity proxies produce very similar RPI estimates. All three proxies indicate that the intensity generally dropped during the IB excursion at this location, but this drop did not occur abruptly and was not completely synchronous with the onset and termination of the inclination anomaly. The initial increase in inclination is associated with an increase in RPI, followed by a fairly abrupt decrease in RPI just before inclinations become negative. As inclinations return to very high values (~ 80–85°), the RPI gradually increases and this gradual increase continues as the inclination anomaly terminates.

The three different palaeointensity proxies, PT-RPI (Fig. 7b), NRM/ARM (Fig. 7c), and NRM/κ (Fig. 7d), for 983B are in excellent agreement and show that the inclination anomaly is accompanied by a highly synchronous drop in RPI. The onset of the excursion is accompanied by a very abrupt decrease in RPI after which the RPI remains constantly low throughout the excursion (~ 25–30% of the non-excursional RPI). The termination of the inclination anomaly is accompanied by an abrupt return to pre-excursional RPI levels. RPI estimates obtained in this study, using PT, NRM/ARM,

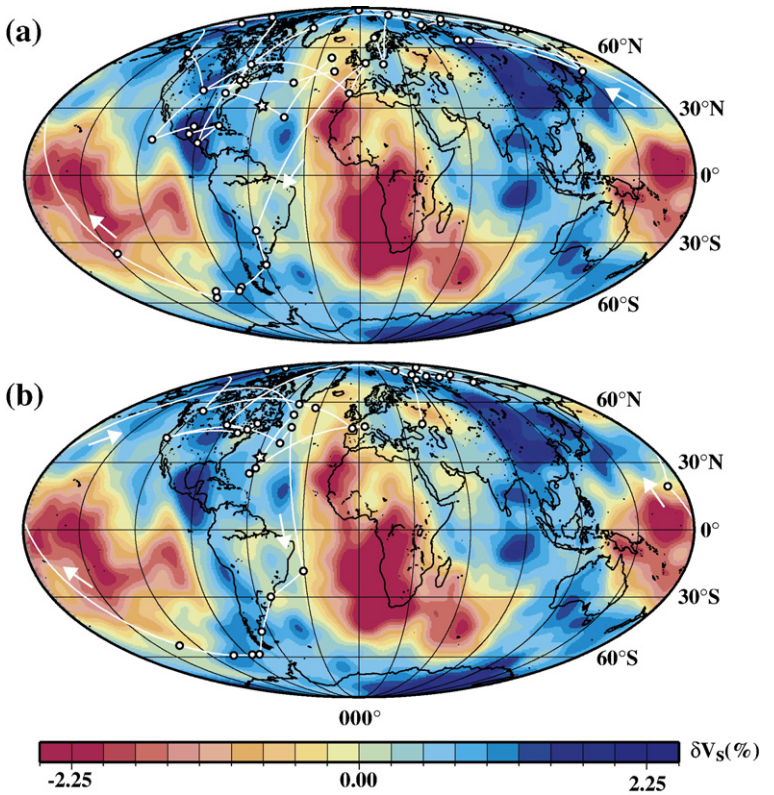

Fig. 8. Virtual geomagnetic poles (VGPs) during the Iceland Basin excursion for (a) 1063A and (b) 1063B. White arrows indicate the direction of the VGP paths and the observation site is indicated with a star. The background map is a tomographic model (SMEAN) of shear-wave velocity anomalies (δV_s) near the CMB (2800 km depth), based on an average of three global intermediate wavelength shear-wave tomography models [49] (image from [50]). Note that blue (red) indicates higher (lower) than average shear-wave velocity.

and NRM/κ as palaeointensity proxies, are in accord with the RPI estimates obtained by Channell [15], who report mean NRM/IRM from U-channels from 983B and 983C.

In both sections 1063A and 983B, we find that RPI estimates obtained using the "brute force" NRM/ARM-method are higher than those obtained with the PT technique. Tauxe et al. [28] observed the same offset and interpreted this as a result of a pervasive VRM biassing the brute force estimates systematically. However, contrary to the observations of Tauxe et al. [28], we find that the degree of offset between the two methods is fairly constant, implying that the NRM/ARM and PT methods provide similar RPI estimates. Other studies indicate a similar agreement between brute force methods and the PT method [29,30], but generally this may not be the case if large variations in the coercivity spectra are present within the studied section.

Despite application of different palaeointensity proxies, several studies indicate that it may be difficult to eliminate influences from environmental changes on the resultant palaeointensity estimates (e.g. [30,15]). The ratio ARM/κ has generally been regarded as a magnetic grain-size proxy, with a decrease in ARM/κ taken to indicate an increase in magnetic grain size. This interpretation, however, may not be straightforward as ARM/κ also is sensitive to the grain-size distribution and clay-mineral content [30]. As shown in Fig. 6e, the relative variations of ARM/κ within the section from 1063A are quite small, and generally do not correlate with variations in palaeointensity. The relative variations of ARM/κ do not provide an explanation for the conspicuous RPI peak observed during the first interval of high inclination values (~ 54.75 mcd), but we suspect that the anomalous PT-RPI and NRM/ARM estimates for the lowermost point may be related to variations in mineralogy. Ratios of ARM/κ are generally constant throughout the section from 983B (Fig. 7e). However, subtle changes within the interval encompassing the large drop in palaeointensity in ARM/κ are detectable, especially close to the termination

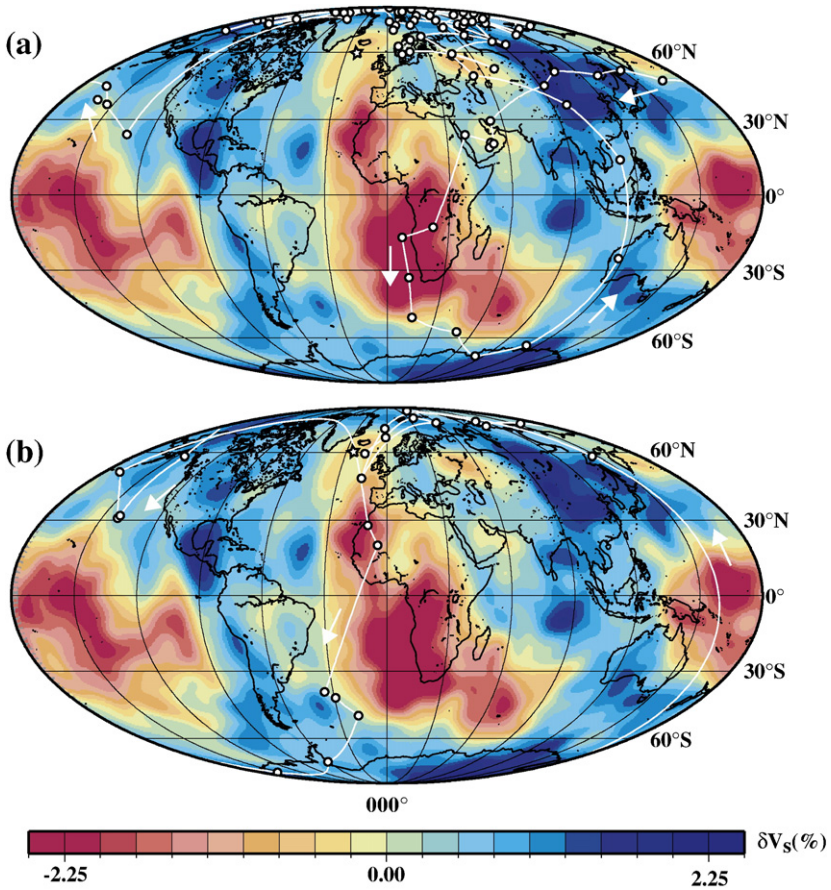

Fig. 9. Virtual geomagnetic poles (VGPs) during the Iceland Basin excursion for (a) 983B and (b) 983C. White arrows indicate the direction of the VGP paths and the observation site is indicated with a star. The background image is the same as in Fig. 8.

of the excursion. Given that the small shift in ARM/κ from pre-excursional levels (~ 300 A/m) to post-excursional levels (~ 400 A/m), similar to the changes observed during the excursion, do not appear to systematically influence the RPI estimates, it seems unlikely that mineralogical changes caused the observed drop in RPI. This is supported by the very high degree of synchronicity between both the onset and termination of the directional anomaly, recorded in both 983B and 983C, and the observed drop in palaeointensity.

5. Discussion

High-resolution records of geomagnetic excursions, such as those from ODP Sites 1063 and 983, render investigations into the behaviour and structure of the excursional field possible. The two new records from Site 1063 present an ideal opportunity to study the behaviour of the geomagnetic field during the IB excursion, because the excursional field is recorded at higher resolution than in any previous record and because inclination and declination data from the two cores are very consistent.

5.1. VGPs from sites 1063 and 983

The VGP paths from Holes 1063A and 1063B (Fig. 8a and b) are in excellent agreement. During the first phase of the IB excursion, VGPs from 1063A and 1063B tend to cluster around the eastern part of North America and the North Atlantic. During this phase of intense downwardly directed field in the Bermuda Rise area, which lasted for ~ 1000 yrs, the VGPs plot close to the observation site. Interestingly, all three palaeointensity proxies indicate an increase in RPI during this initial phase. Somewhat similarly, the field intensity before or just after completion of a reversal has been observed to temporarily overshoot the normal value for full polarity by up to 50% [33–35]. The first phase is followed by a period of very rapid field changes after which the VGPs are found to cluster around the southern tip of South America. Prior to this apparent jump in VGP position, the RPI decreases to a minimum before increasing slightly during the period where the VGPs linger around the tip of South America. This clustering of VGPs in the southern hemisphere is followed by another period of very rapid field change during which the VGPs return to the area around the eastern part of North America (note that the interval between samples, during which the periods of rapid field change take place, is as small as 1.5 cm). Here they remain for ~ 1000 yrs before finally returning to higher latitudes as the excursion ends. The second period of rapid field change coincides with another minimum in RPI, which from this point increases gradually towards and beyond the termination of the excursion.

VGP paths from Holes 983B and 983C (Fig. 9a and b) do not agree as well as the VGP paths from Site 1063, mainly because of differences in declination during the excursion. However, both VGP paths seem to agree on the overall trend during the excursion. The first part of the IB excursion is defined by an abrupt change from normal field directions to VGPs plotting off the Californian coast in the eastern Pacific. Subsequently, the VGPs from 983B cross the Pacific, continue through Asia and Africa to complete a very well-defined counterclockwise loop around the rim of the Indian ocean, before returning through Asia to high latitudes as the excursion ends. The VGP path for 983C is much less well-defined than the path for 983B. Subsequent to the initiation of the excursion, defined by VGPs plotting in the eastern Pacific, the VGPs from 983C track down the Atlantic and western part of Africa to the South Atlantic, where they briefly seem to cluster, before returning abruptly to high northern latitudes via Northeast Asia. The VGP paths observed in this study are generally very similar to the VGP paths observed in the U-channel records by Channell [15]. The initiation of the excursion is accompanied by a synchronous and very abrupt drop in RPI, which remains at a constant, low level throughout the excursion before abruptly returning to pre-excursional levels as the VGPs return to high northern latitudes. It is noteworthy that the return to pre-excursional RPI levels is less abrupt than the drop observed at the onset of the excursion.

5.2. Existence of intense patches of vertical flux

It has been suggested that transitional VGPs associated with polarity reversals preferentially lie within two nearly antipodal bands, one passing through the Americas and the other through western Australia and eastern Asia [36,37]. This suggestion was contested in several subsequent studies [38–40], but detailed statistical analyses later indicated that intermediate VGPs from reversals, and possibly also excursions, tend to fall along American and Austral-Asian longitudes, roughly consistent with the original observations from sediment records [41,42]. This issue, which remains a subject of strong debate within the palaeomagnetic community, is important since presence of persistent non-axisymmetric components in transitional fields would imply that the core and mantle are dynamically coupled [41,43]. It is therefore noteworthy that most of the excursional VGPs

from 1063A and 1063B in this study tend to fall along American longitudes (Fig. 8a and b). The first part of the VGP path from Site 983 do not coincide with the preferred palaeomagnetic longitudes, whereas the latter part tends to track along the preferred band over western Australia and East Asia (Fig. 9a and b).

More specifically, VGPs from 1063A and 1063B seem to cluster within or close to two of the preferred VGP-cluster patches suggested by Hoffman [8]. Hoffman [8] argued that the transitional field displays rapid stop-and-go movements between metastable transitional-field states that are related to long-standing thermodynamic features of the core–mantle system. The transitional field will then spend most of its time within one of these hang-up points [8], which tend to coincide with regions of high seismic velocity in the lower mantle [44,45]. Comparison of the VGPs from Site 1063 with S-wave tomography of the lowermost mantle, shows that the VGPs generally fall within regions of high seismic-shear-wave velocity (δV_s) just above the CMB, and that the VGP clusters tend to coincide with regions of maximum seismic-shear-wave velocity under North America and the southernmost South America (Fig. 8). During the beginning and termination of the excursion, there is a slight tendency for the VGPs from 983B to hover around the Northeast-Asia cluster patch of Hoffman [8], a region coinciding with a strong maximum in δV_s (Fig. 9). However, it is noteworthy that part of the VGP path from 983B falls within a large region of low seismic velocity under Africa.

VGPs from 1063 indicate that the field at this location was dominated by patches of intense vertical flux, which possibly caused a brief increase in intensity during the first phase of the excursion. Numerical simulations of tomographic geomagnetic reversals, where the heat flux over the core–mantle boundary varies according to seismic velocities in the lowermost mantle, suggest that strong, localised patches of vertical flux can develop in less than a 100 yrs during a reversal, and that they are associated with extremely high non-dipole fields [11]. It is intriguing that the cluster patch observed around the tip of South America in this study also coincides with a reverse-flux feature (a patch of flux of opposite sign to that expected for a dipole field) in the present field at the core–mantle boundary beneath South America [46,47]. Such reverse-flux features are believed to arise from flux expulsion from the core, caused by upwelling associated with higher-than-average heat flux across the CMB. It has been suggested that development and poleward propagation of such reverse-flux patches can lead to a polarity reversal [47]. Based on the high-resolution data recorded at Site 1063, we speculate that a similar, but perhaps more intense, reverse-flux feature could have developed and contributed to the decline of the axial dipole during the IB excursion. For some reason, perhaps because of a limited duration, conditions were not favourable for the excursion to develop into a full polarity reversal.

5.3. Comparison of VGP paths

Comparison of VGPs from Site 1063 (Fig. 8a and b) and Site 983 (Fig. 9a and d) reveal some notable differences in the VGP paths from the two sites, especially when the VGP path from 983B is compared to those from 1063. It is quite clear that the field observed at Site 983 during the IB excursion was not dominated by the same patches of vertical flux that dominated the field at Site 1063. In turn, this could explain the differences in the RPI observed at Sites 1063 and 983. The brief increase and general absence of an abrupt decrease in RPI at 1063A might thus be caused by the proximity of the observation site to one of the patches of strong vertical flux, whereas the RPI from 983B not is affected by these flux patches. The different VGP paths from Sites 1063 and 983 suggest that the global geomagnetic field was not dominated by a simple dipole during the IB excursion. Based on observations in this study from only two locations, it is impossible to ascertain whether the field retained a fairly simple structure during the excursion or whether it was dominated by a more complex morphology, such as four-fold symmetry [48,43]. Several records of the IB excursion have been reported in the literature [16–20,4,21], but the majority of these did not record the excursion in sufficient detail to resolve the excursional field behaviour. We note that a VGP-path morphology reasonably similar to that observed for the IB excursion from Site 983 in this study, was observed for the same excursion by Oda et al. [17] in Lake Baikal sediments (53.7°N, 108.4°E) with an average sedimentation rate of 4.3 cm kyr^{-1}. To fully understand the field structure during the IB excursion, it is essential to obtain more high-resolution records from geographically dispersed locations.

6. Conclusions

The new records of the Iceland Basin excursion from ODP Holes 1063A and 1063B, and from ODP Holes 983B and 983C, provide the highest resolution records obtained so far for this excursion. The two records from Site 1063 on the Bermuda Rise are in excellent agreement and the inclination records show that the excursion peak was both preceded and succeeded by a conspicuous interval of very high inclinations. The two records from

Site 983 in the far North Atlantic are generally in good agreement, although the inclination anomalies are more consistent than the declination anomalies.

RPI estimates were obtained from Sites 1063 and 983 using both the pseudo-Thellier technique and more conventional methods (NRM/ARM and NRM/κ). At Site 1063 the RPI generally decreased during the excursion, but the intensity changes were fairly gradual and the RPI may have increased briefly during the beginning of the excursion. At Site 983, the field experienced a very abrupt decrease in RPI synchronous with a rapid change in geomagnetic field directions. The RPI remained at a constant, low level throughout the excursion before returning to high pre-excursional levels synchronous with the termination of the directional anomaly.

VGPs from Site 1063 indicate that the excursional field during the IB excursion was dominated by seemingly metastable patches of vertical flux over North America and the tip of South America. The field appears to have experienced some stop-and-go behaviour between these flux patches, which coincide reasonably well with the preferred longitudes of palaeomagnetic VGPs and zones of high seismic velocity in the lower mantle. One of these flux patches was associated with a conspicuous increase in RPI. VGPs from 983B track along a different path, which partly coincides with the preferred palaeomagnetic VGP path over western Australia. The different VGP paths from Sites 1063 and 983 indicate that the global field structure during the IB excursion was not dominated by a single dipole. More records with resolution as high as those presented here are needed to assess the geomagnetic field structure during the IB excursion.

Acknowledgements

The ARM acquisitions were carried out in the Palaeomagnetic and Mineral Magnetic Laboratory at the GeoBiosphere Science Centre, University of Lund, Sweden. Rob Van der Voo and Peter Riisager provided helpful comments on an early draft of this manuscript. Critical reviews by Carlo Laj, Cor Langereis, Trond Torsvik, and two anonymous referees greatly improved the manuscript. M.F. Knudsen is grateful for financial support from the Danish National Science Foundation, STOPFEN and a Marie Curie Intra-European Fellowship (MEIF-CT-2005-011034). Conall Mac Niocaill and Gideon M. Henderson were supported by NERC grants NER/T/S/2000/00039 and NER/T/S/2003/00041.

Appendix A. Supplementary data

Supplementary data associated with this article can be found, in the online version, at doi:10.1016/j.epsl.2006.08.016.

References

[1] S.P. Lund, T. Williams, G.D. Acton, B. Clement, M. Okada, Brunhes Chron magnetic field excursions recovered from Leg 172 sediments, Proc. Ocean Drill. Program Sci. Results 172 (2001) 1–18.

[2] C. Laj, C. Kissel, A. Mazaud, J.E.T. Channell, J. Beer, North Atlantic palaeointensity stack since 75ka (NAPIS-75) and the duration of the Laschamp event, Phil. Trans. R. Soc. Lond. 358 (2000) 1009–1025.

[3] C. Kissel, C. Laj, L. Labeyrie, T. Dokken, A. Voelker, D. Blamart, Rapid climatic variations during marine isotopic stage 3 magnetic analysis of sediments from Nordic Seas and North Atlantic, Earth Planet. Sci. Lett. 171 (1999) 489–502.

[4] N.R. Nowaczyk, M. Antonow, High-resolution magnetostratigraphy of four sediment cores from the Greenland Sea-I. Identification of the Mono Lake excursion, Laschamp and Biwa I/Jamaica geomagnetic polarity events, Geophys. J. Int. 131 (1997) 310–324.

[5] D. Gubbins, The distinction between geomagnetic excursions and reversals, Geophys. J. Int. 137 (1999) F1–F3.

[6] R. Hollerbach, C.A. Jones, Influence of the Earth's inner core on geomagnetic fluctuations and reversals, Nature 365 (1993) 541–543.

[7] G.A. Glatzmaier, R.S. Coe, L. Hongre, P.H. Roberts, The role of the Earth's mantle in controlling the frequency of geomagnetic reversals, Nature 401 (1999) 885–890.

[8] K.A. Hoffman, Dipolar reversal states of the geomagnetic field and core–mantle dynamics, Nature 359 (1992) 789–794.

[9] B.M. Clement, Dependence of the duration of geomagnetic polarity reversals on site latitude, Nature 428 (2004) 637–640.

[10] B. Singer, K.A. Hoffman, R.S. Coe, L.L. Brown, B.R. Jicha, M.S. Pringle, A. Chauvin, Structural and temporal requirements for geomagnetic field reversal deduced from lava flows, Nature 434 (2005) 633–636.

[11] R.S. Coe, L. Hongre, G.A. Glatzmaier, An examination of simulated geomagnetic reversals from a palaeomagnetic perspective, Phil. Trans. R. Soc. Lond. 358 (2000) 1141–1170.

[12] J. Wicht, Palaeomagnetic interpretation of dynamo solutions, Geophys. J. Int. 162 (2005) 371–380.

[13] A.P. Roberts, M. Winklhofer, Why are geomagnetic excursions not always recorded in sediments? Constraints from post-depositional remanent magnetisation lock-in modelling, Earth Planet. Sci. Lett. 227 (2004) 345–359.

[14] J.E.T. Channell, D.A. Hodell, B. Lehman, Relative paleomagnetic intensity and δ^{18}O, Earth Planet. Sci. Lett. 153 (1997) 103–118.

[15] J.E.T. Channell, Geomagnetic paleointensity and directional secular variation at Ocean Drilling Program (ODP) Site 984 (Bjorn Drift) since 500 ka: comparisons with ODP Site 983 (Gardar Drift), J. Geophys. Res. 104 (1999) 22937–22951.

[16] J.S. Stoner, J.E.T. Channell, D.A. Hodell, C.D. Charles, A ~ 580 kyr geomagnetic paleosecular variation record from the

sub-Antarctic South Atlantic (Ocean Drilling Program Site 1089), J. Geophys. Res. 108 (B5) (2003) doi:10.1029/2001JB001390.
[17] H. Oda, K. Nakamura, K. Ikehara, T. Nakano, M. Nishimura, O. Khlystov, Paleomagnetic record from Academician Ridge, Lake Baikal: a reversal excursion at the base of marine oxygen isotope stage 6, Earth Planet. Sci. Lett. 202 (2002) 117–132.
[18] A.P. Roberts, B. Lehmann, R.J. Weeks, K.L. Verosub, C. Laj, Relative paleointensity of the geomagnetic field over the last 200,000 years from ODP Sites 883 and 884, North Pacific Ocean, Earth Planet. Sci. Lett. 152 (1997) 11–23.
[19] B. Lehmann, C. Laj, C. Kissel, A. Mazaud, M. Paterne, L. Labeyrie, Relative changes of the geomagnetic field intensity during the last 280 kyear from piston cores in the Açores area, Phys. Earth Planet. Inter. 93 (1996) 269–284.
[20] R.J. Weeks, C. Laj, L. Endignoux, A. Mazaud, L. Labeyrie, A.P. Roberts, C. Kissel, E. Blanchard, Normalised natural remanent magnetisation intensity during the last 240 000 years in piston cores from the central North Atlantic Ocean: geomagnetic field intensity or environmental signal? Phys. Earth Planet. Inter. 87 (1995) 213–229.
[21] T. Yamazaki, N. Ioka, Long-term secular variation of the geomagnetic field during the last 200 kyr recorded in sediment cores from the western equatorial pacific, Earth Planet. Sci. Lett. 128 (1994) 527–544.
[22] E.P. Laine, W.D. Gardner, M.J. Richardson, M.A. Kominz, Abyssal currents and advection of resuspended sediment along the northeastern Bermuda Rise, Mar. Geol. 119 (1994) 159–171.
[23] J.E.T. Channell, A. Mazaud, P. Sullivan, S. Turner, M.E. Raymo, Geomagnetic excursions and paleointensities in the Matuyama Chron at Ocean Drilling Program Sites 983 and 984 (Iceland Basin), J. Geophys. Res. 107 (2002) EPM1–EPM11.
[24] J. Imbrie, J.D. Hays, D.G. Martinson, A. McIntyre, A.C. Mix, J.J. Morley, W.L. Prell, N.G. Pisias, N.J. Shackleton, in: A.L. Berger, et al., (Eds.), Milankovitch and Climate, Part I, Reidel, The Netherlands, 1984, pp. 269–305.
[25] D.G. Martinson, N.G. Pisias, J.D. Hays, J. Imbrie, T.C. Moore Jr., N.J. Shacketon, Age dating and the orbital theory of the ice ages: development of a high-resolution 0 to 300,000-year chronostratigraphy, Q. Res. 27 (1987) 1–29.
[26] Shipboard Scientific Party (Site 1063), Proc. Ocean Drilling Program, Initial Rep. 172 (1998) 251–308.
[27] Shipboard Scientific Party (Site 983), Proc. Ocean Drilling Program, Scientific Results 162 (1999) CD-ROM.
[28] L. Tauxe, T. Pick, Y.S. Kok, Relative paleointensity in sediments: a pseudo-Thellier approach, Geophys. Res. Lett. 22 (1995) 2885–2888.
[29] I. Snowball, P. Sandgren, Geomagnetic field intensity changes in Sweden between 9000 and 450 cal BP: extending the record of "archaeomagnetic jerks" by means of lake sediments and the pseudo-Thellier technique, Earth Planet. Sci. Lett. 227 (2004) 361–376.
[30] P.P. Kruiver, Y.S. Kok, M.J. Dekkers, C.G. Langereis, C. Laj, A pseudo-Thellier relative palaeointensity record, and rock magnetic and geochemical parameters in relation to climate during the last 276 kyr in the Azores region, Geophys. J. Int. 136 (1999) 757–770.
[31] R.S. Coe, S. Grommé, E.A. Mankinen, Geomagnetic paleointensities from radiocarbon-dated lava floes on Hawaii and the question of the Pacific nondipole low, J. Geophys. Res. 83 (1978) 1740–1756.
[32] L. Sagnotti, F. Budillon, J. Dinares-Turell, M. Iorio, P. Macri, Evidence for a variable paleomagnetic lock-in depth in the Holocene sequence from the Salerno Gulf (Italy): Implications for "high-resolution" paleomagnetic dating, Geochem. Geophys. Geosyst. 3 (2005) doi:10.1029/2005GC001043.
[33] M. Prévot, E.A. Mankinen, C.S. Coe, R.S. Grommé, How the geomagnetic field vector reverses polarity, Nature 316 (1985) 230.
[34] M. Prévot, E. Mankinen, C. Coe, R.S. Grommé, The Steens Mountain (Oregon) geomagnetic polarity transition. 2. Field intensity and discussion of reversal models, J. Geophys. Res. 90 (1985) 10417–10448.
[35] S.W. Bogue, R.T. Merrill, The character of the field during reversals, Annu. Rev. Earth Planet. Sci. 20 (1992) 181–219.
[36] B.M. Clement, Geographical distribution of transitional VGP's: evidence for nonzonal equatorial symmetry during the Matuyama–Brunhes geomagnetic reversal, Earth Planet. Sci. Lett. 104 (1991) 48–58.
[37] C. Laj, A. Mazaud, R. Weeks, M. Fuller, E. Herrero-Bervera, Geomagnetic reversal paths, Nature 351 (1991) 447.
[38] G.D. Egbert, Sampling bias in VGP longitudes, Geophys. Res. Lett. 19 (1992) 2353–2356.
[39] J.-P. Valet, P. Tucholka, V. Courtillot, L. Meynadier, Paleomagnetic constraints on the geometry of the geomagnetic field during reversals, Nature 356 (1992) 400–407.
[40] C.G. Langereis, A.A.M. van Hoof, P. Rochette, Longitudinal confinement of geomagnetic reversal paths as a possible sedimentary artefact, Nature 358 (1992) 226–230.
[41] J.J. Love, Paleomagnetic volcanic data and geometric regularity of reversals and excursions, J. Geophys. Res. 103 (B6) (1998) 12435–12452.
[42] J.J. Love, Statistical assessment of preferred transitional VGP longitudes based on palaeomagnetic lava data, Geophys. J. Int. 140 (1) (2000) 211–221.
[43] D. Gubbins, J.J. Love, Preferred VGP paths during geomagnetic polarity reversals: symmetry considerations, Geophys. Res. Lett. 25 (1998) 1079–1082.
[44] A.M. Dziewonski, J. Woodhouse, Global images of the Earth's interior, Science 236 (1987) 37–48.
[45] B. Romanowicz, 3D structure of the Earth's lower mantle, C.R. Geosci. 335 (2003) 23–35.
[46] J. Bloxham, D. Gubbins, The secular variation of the Earth's magnetic field, Nature 317 (1985) 777–781.
[47] D. Gubbins, Mechanism for geomagnetic polarity reversals, Nature 326 (1987) 167–169.
[48] D. Gubbins, G. Sarson, Geomagnetic reversal transition paths from a kinematic dynamo model, Nature 368 (1994) 51–55.
[49] T.W. Becker, L. Boschi, A comparison of tomographic and geodynamic mantle models, Geochem. Geophys. Geosyst. 3 (2002) doi:10.1029/2001GC000168.
[50] K. Burke, T.H. Torsvik, Derivation of large igneous provinces of the past 200 million years from long-term heterogeneities in the deep mantle, Earth Planet. Sci. Lett. 227 (2004) 531–538.